

INVESTIGATING PAPER CURL BY SHEET SPLITTING

Ulrich Hirn and Wolfgang Bauer

Graz University of Technology

Institute of Pulp-, Paper- and Fiber Technology

Kopernikusgasse 24, 8010 Graz, Austria

ulrich.hirn@tugraz.at

wolfgang.bauer@tugraz.at

Abstract

First the theory of paper curl and the literature of curl related paper testing is briefly reviewed. Based on the theory quantitative models for the influence of fiber orientation two sidedness and paper hygroexpansivity on curl are given. It has to be pointed out that fiber orientation affects CD curl and diagonal curl in different ways: CD curl is promoted by FO *anisotropy* two-sidedness but diagonal curl is promoted by FO *angle* two-sidedness.

In the second part of the article industrial copy paper with curl problems is analyzed using the model equations. Fiber orientation across the z-direction of the copy papers is measured using a sheet splitting method and hygroexpansivity is determined using an ultrasonic sheet tester.

Curl behavior of the paper is well described by the model equations. In particular it can be explained, why the CD curl and the diagonal curl in the examined papers show great differences. Thus the outlined analysis procedure, i.e. measurement of z-directional FO measurement and hygroexpansivity, may help to evaluate interrelations between fiber orientation and curl of industrial papers with curl problems.

1 Theory of paper curl

A concise yet exhaustive summary of technological influences as well as fundamental reasons for curl can be found in [KAJANTO & NISKANEN 1998]. A thorough review of curl literature and results of a quantitative curl model is also given by [FEICHTINGER 1996].

Curl refers to large scale out of planeness of paper. The paper is deformed to a bowl or cylinder shape. Curl is composed of three independent components K_x , K_y and K_{xy} which together form the total curl, see figure 1. Curl is generally caused by z-directional inhomogeneities in swelling or shrinkage of the paper. Consider a sheet, where one surface shrinks, the other one

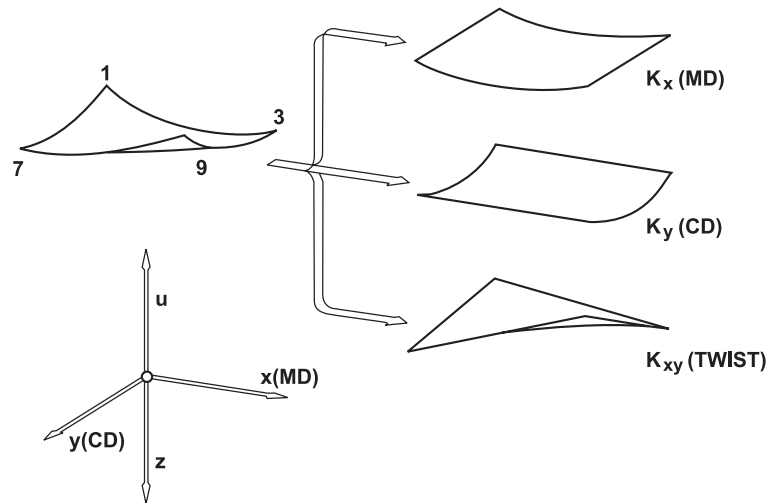


Figure 1 Sheet curl consists of three independent components: MD-Curl K_x , CD Curl K_y and diagonal curl K_{xy} [LEVLIN & SÖDERHJELM 1999].

does not. This will result in internal stresses which are released by curling of the sheet towards the shrinking side. Generally there are two different reasons for curl

- inhomogeneous drying or moistening
- z-directional differences in hygroexpansivity

Inhomogeneous drying or moistening. If paper is dried only on one side, the two paper sides are not shrinking synchronously. As a result the paper curls towards the surface through which moisture was last removed from the sheet [KAJANTO & NISKANEN 1998]. One sided drying also occurs in laser printing and copying. Usually this effect is not strong enough to actually *cause* paper curl, but it may amplify z-directional differences in hygroexpansivity.

Inhomogeneous moistening is quite frequent in printing of paper or may occur during coating or converting, eventually leading to curl problems.

Z-directional differences in hygroexpansivity. Fibers are hygroexpansive, they swell and shrink upon changes in relative humidity. So all factors promoting the hygroexpansivity of paper usually promote curl problems. Such factors are for example degree of beating, filler content and fiber type (fibers with high lignin content have less dimensional changes). Another major influence factor on hygroexpansivity is drying shrinkage. Paper that was dried without tension shrinks. The larger the drying shrinkage, the larger is the dimensional change following variations in humidity [KAJANTO & NISKANEN 1998]. High draw in the drying section reduces web shrinkage and thus dimensional instability. Still shrinkage is much stronger towards the web edges, so paper from the edge zones of the web are more prone to curl [SHANDS &

GENCO 1988]. Apart from overall shrinkage which *promotes* curl, z-directional differences in shrinkage *cause* curl. However, the situation is totally different for diagonal curl and CD curl.

Diagonal Curl is always related to fiber orientation. The most important cause is two sidedness of the fiber orientation angle. A quantitative model equation is given by [NISKANEN 1993]

$$K_{xy} = \frac{2(\phi_{TS} - \phi_{BS})(H_{MD} + H_{CD})}{t}. \quad (1)$$

K_{xy} is the intensity of the diagonal curl and $\phi_{TS} - \phi_{BS}$ is the difference of fiber orientation angle between top side and bottom side. H_{MD} respectively H_{CD} denote the hygroexpansivity in MD and CD, finally t is sheet caliper. According to equation (1) diagonal curl is composed of two independent causes, FO angle two-sidedness and hygroexpansivity. The underlying reason for this is, that upon changes in relative humidity fibers shrink about 1% longitudinally but up to 20% laterally. Therefore if the fibers are not aligned in the same angle on top and bottom side of the sheet, the two sheet halves have different main directions of expansion/shrinkage. This leads to inner tensions and subsequent diagonal curl. Anisotropy of fiber orientation does not appear in expression (1), however at least in one half of the sheet must be some anisotropy otherwise the sheet expands isotropically and no curl emerges.

For thin papers (i.e. a grammage around 50 g/m²) there is evidence, that diagonal curl descends from high overall FO anisotropy in the sheet [VIITAHARJU & NISKANEN 1994]. All wood fibers have the same right handed chirality of the cellulose fibrils in the S2 fiber wall. This chirality causes a slight bending in the same direction upon humidity changes, which is said to be the cause for diagonal curl of thin papers.

CD Curl. A general model for curl based on differential shrinkage in different layers of a plate describe [CARLSSON ET AL. 1980]. A simplified version is given by [SHANDS & GENCO 1988], according to this equation curl simply depends on the difference in top- and bottom side CD strain

$$K_y = \frac{2(\varepsilon_{CD}^{TS} - \varepsilon_{CD}^{BS})}{t}. \quad (2)$$

ε_{CD}^{TS} denotes the CD strain in the top side of the sheet, ε_{CD}^{BS} is the CD strain in the bottom side. There may be many reasons for differential CD strain. A quite frequent cause is FO anisotropy two-sidedness together with strong hygroexpansivity in cross direction. Although hygroexpansivity does not directly show up in equation (2), it must be stressed that it is the primary reason for the CD strain ε_{CD} . Furthermore all one sided drying and moistening processes (like for example copying) usually produce CD curl. The reason for that is that paper normally shrinks more in CD than in MD due to fiber orientation. So one sided drying produces differential CD shrinkage which promotes CD curl.

The curl models described here are based on major simplifications. More complex behavior of curl has been reported for instance by [ODELL & PAKARINEN 2000]. They described a paper with heavy CD curl. It had strong FO anisotropy two-sidedness, the top side being oriented more intensely. Switching from drag to rush, the anisotropy two-sidedness flipped, now the bottom side being more oriented. From theory, it should be expected that the CD curl would prevail, only the sheet would bend towards the other surface. However, the sheet bent towards the same surface, but the curl mode changed from CD-curl towards MD curl. With zero speed difference the paper exhibited diagonal curl. So it is important to keep in mind, that the curl models discussed before, have been simplified and thus are not universally valid.

2 Curl related paper testing

As discussed above, hygroexpansivity and fiber orientation are the main reasons for curl. Therefore analysis of curled paper focuses on these two parameters.

Assessment of **drying tensions in the paper** perform [LLOYD & CHALMERS 2001]. They measure the difference between MD/CD ratios of sheet splitting fiber orientation and ultrasonic tensile stiffness. Tensile stiffness incorporates FO anisotropy *and* drying tensions [LINDBLAD & FÜRST 2001] so differences between these two MD/CD ratios give an indication about the drying tensions in the paper.

[NISKANEN 1993] pointed out, that shrinkage of the web is caused by two independent factors, namely wet straining and drying shrinkage. He provides data illustrating, that for wood containing paper grades total shrinkage is to equal parts caused by wet straining and drying, for wood free papers shrinkage occurs predominantly in drying. The key point is that **only drying shrinkage is directly related to hygroexpansivity** of paper, and thus to dimensional instability. So shrinkage measurement methods that determine drying shrinkage, as for example the ultrasonic method, give more relevant information regarding curl than methods that measure total shrinkage (like the wire mark shrinkage method). Ultrasonic testing for investigation of CD shrinkage in curled papers is for instance used by [SHANDS & GENCO 1988].

Sheet splitting based measurement of **z-directional hygroexpansivity** for curled paper samples is reported by [GREEN 2000]. Specimen are split in two layers and the changes in sample length for varied relative humidity are measured. So the method directly measures the difference of dimensional changes in the top and bottom halve of the sheet. Measurement of fiber orientation in the split layers could provide additional useful information.

Z-directional fiber orientation is evaluated in many publications dealing with paper curl. For example [KNOTZER ET AL. 2003] measured z-directional FO with sheet splitting on curled copy paper, finding considerable angle two-sidedness. [LLOYD & CHALMERS 2001] also eval-

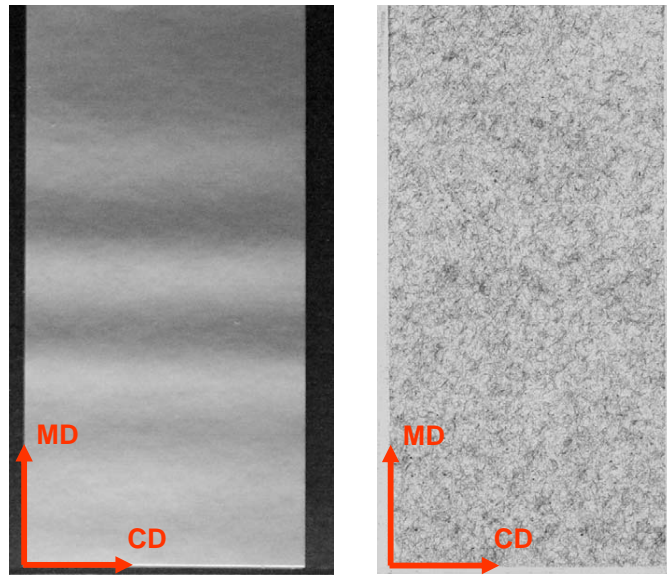


Figure 2 The contours of the specimen (left) are well visible in the split layers (right). By defining a coordinate system determined by the sample edges, the position of individual fibers in the split layers can be mapped to the original position in the sheet. Sample size is $3.6 \times 7 \text{ cm}^2$.

uated layered fiber orientation across the z-direction of curled and flat papers. They found considerably higher FO angle and anisotropy two-sidedness in the curled paper sheets. Additionally they analyzed local variability of the FO angle in different layers of the sheet. Higher variation in FO angle was found in the layers where the FO angle showed severe misalignment from MD. They attribute this to vibrations in the forming zone and speculate, that these vibrations might be related to the FO angle misalignment. Fiber orientation two-sidedness of curled copy paper is also evaluated by [NISKANEN 1993] using an optical surface fiber orientation sensor.

The influence of an uneven **z-directional elastic modulus (Young's modulus)** on heat curl of newsprint is investigated by [MORRIS & SAMPSON 1998]. Sheets are split with the Beloit sheet splitter, the elastic modulus in the split layers is determined using Tappi method T-535 cm85 (stiffness of paperboard-resonance length method). Although their data is quite noisy, the results indicate, that papers with large two-sidedness in the MD/CD ratio of the in-plane elastic modulus have stronger curl. Considering these interesting findings it might be worthwhile using an ultrasonic instrument for measurement of the elastic modulus instead of the Tappi method, as this should definitely provide less noisy data.

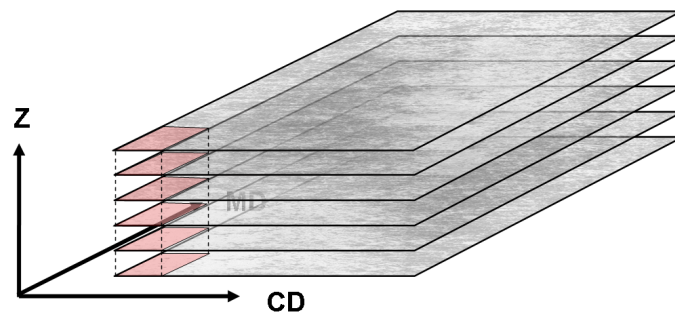


Figure 3 A three dimensional model is obtained by defining a coordinate system by the sample edges in individual layers and subsequent stacking of the FO data layers.

3 Measuring 3-Dimensional Layered Fiber Orientation

This section describes a z-directional fiber orientation measurement method developed at the Institute of Pulp-, Paper- and Fiber Technology within the last years [HIRN 2006]. It is based on a sheet splitting FO measurement method originally developed by [KNOTZER ET AL. 2003].

Image 2 (left side) shows a paper sample as it is used for measurement of local fiber orientation. The sample has a strictly defined geometry, it is rectangular and has a size of $3.6 \times 7 \text{ cm}^2$. Specimens are cut using a punch, this way it is ensured that they have equivalent geometry. A sample is split into 80-150 layers, see section 3.1. The fibers in each split layer are well visible see figure 2, right image. This image also shows, that the outline of the paper sample is clearly visible in the split layer. Using two edges of the sample as coordinate axes the exact position of each analyzed fiber in every layer can be defined. The coordinate system in each layer is equivalent to the edges of the original sample so the MD-CD position of each analyzed fiber is unambiguously determined.

The sheet is split and the fiber orientation in the individual layers is measured as described in section 3.2. Then a three-dimensional model of fiber orientation is formed by stacking the FO data obtained from all layers. Having obtained the three dimensional data of fiber orientation, FO distributions from arbitrary volume sections within the model can be aggregated. From these distributions fiber orientation angle and anisotropy are computed. For example by taking all fibers within defined subareas of the sample, *local fiber orientation* can be determined, see figure 4(a). In this image the fiber orientation distribution of local subareas sized $3.6 \times 3.6 \text{ mm}^2$ is displayed as an approximated ellipse. Image 4(b) gives a different visualization of the same sample. The FO angle is now plotted for three different views of the sample, top view MD-CD, front view CD-z and side view MD-z. The top view, MD-CD, gives the local FO angle equivalent to figure 4(a). The other views, CD-z and MD-z, are cross sections through the thickness direction of the sheet. In the paper cross sections displayed in image 4(b) a clearly

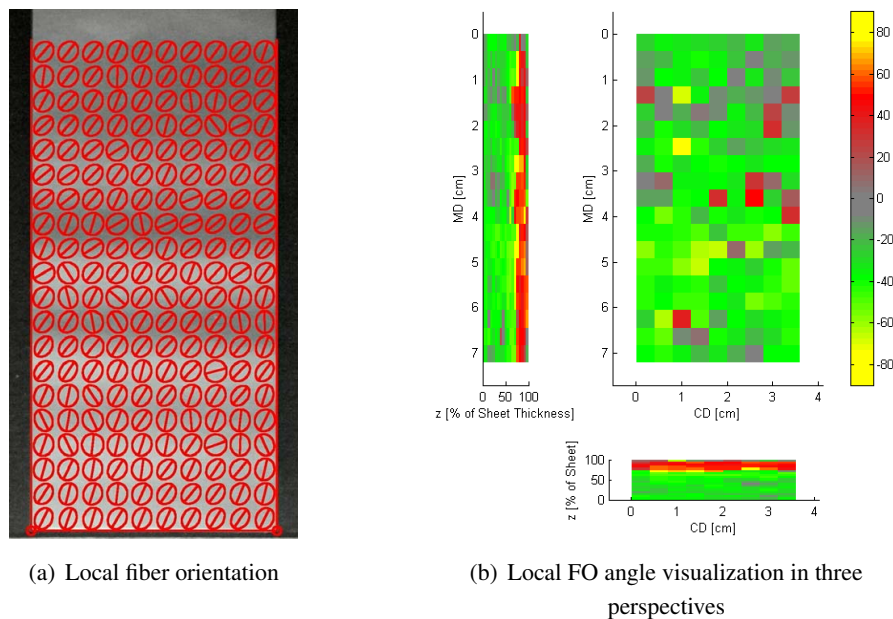


Figure 4 Two visualization techniques for local fiber orientation. Both images show the FO data for the paper specimen displayed in figure 2.

discernible red region in the top 60% of the sheet indicates a disruption in the fiber orientation on the top side of the paper.

3.1 Sheet Splitting

Before the sample is split, it is dyed for improved contrast of the fibers in the subsequent imaging process. We use Cartaren Black, a cationic dye from Clariant. In a laboratory trial it proved to be superior, mainly because it penetrates very well into the paper. In fact even heavily coated papers are dyed entirely and can be split with our method.

For splitting [KNOTZER ET AL. 2003] the sheet is laminated in a commercial hot laminator with temperature control, as it can be bought from office suppliers. Then the sample can be split in two halves by hand as illustrated in figure 5. By repeating this procedure the paper is split to increasingly thin layers, usually to $\sim 1 \text{ g/m}^2$, that is 60-100 layers for an 80 g/m^2 paper. With this technique layers with only a few fibers per mm^2 can be obtained, for some experiments layers covered with as little as 0.4 g/m^2 were produced.

For most sheet splitting methods the sample is fixed on two rolls and split in the outgoing roll nip, as for example in the Beloit Sheet Splitter [PARKER & MIH 1964]. Such a procedure reduces the influence of laboratory personnel manually performing the split. However we found,

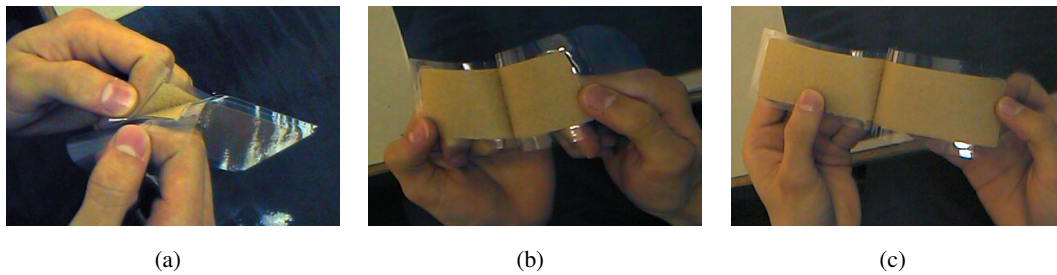


Figure 5 Sheet splitting from paper laminates. Both paper surfaces adhere to the laminating film and the sheet is torn in two layers.

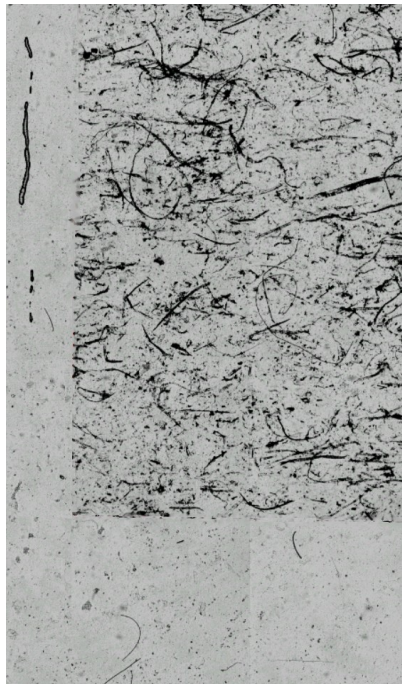
that the influence of manual splitting on the result is low. Experiments regarding this issue are treated in detail in [HIRN 2006]. In summary the influence of dyeing and splitting on the measured fiber orientation is remarkably low for unoriented sheets (handsheets). For oriented sheets it is strictly recommended to lead the splitting movement in machine direction. Although splitting in cross direction does preserve the principal characteristics of the FO in the sheet, it repositions the fibers systematically.

The method was evaluated extensively [HIRN 2006]. Reference measurements with other sheet splitting methods [ERKKILÄ ET AL. 1998] as well as a surface fiber orientation measurements [NEMETH ET AL. 1999] showed good agreement. The method has also been employed for analysis of cockling and finger ridging [HIRN ET AL. 2004].

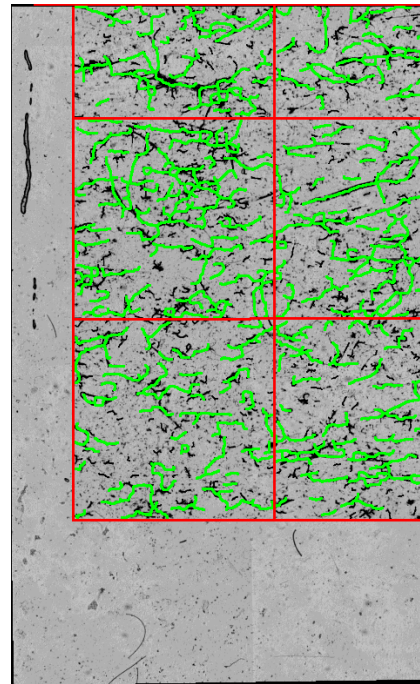
3.2 Fiber Orientation Measurement with Image Analysis

The fibers in the split layers are suspended between two sheets of transparent laminating foil. They are well visible under backlight illumination, see image 6(a). In the first step the fiber layers are scanned at a resolution of 3300 dpi. This can be done with a microscope equipped with an automated scanning stage and a CCD camera or a high resolution film scanner. The scanner delivers better images and it is also faster, so usually the scanner is chosen.

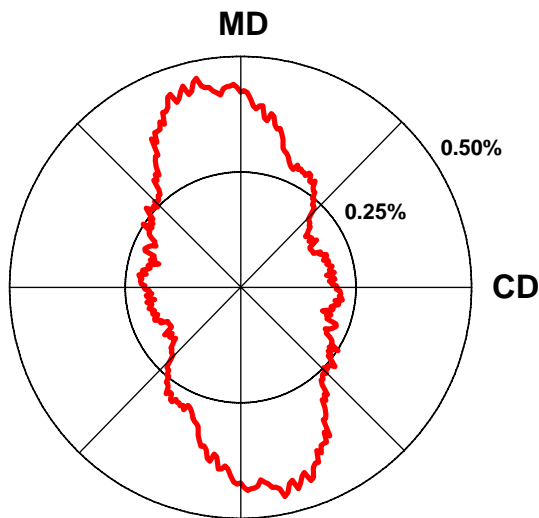
In the photographed images the operator interactively marks the sample edges, then the image is processed. Image analysis [HIRN 2006] detects the centerlines of all fibers and fiber parts longer than $170 \mu\text{m}$, see image 6(b). For fiber orientation measurement these centerlines are first approximated by polygons with a segment length of $130 \mu\text{m}$. Then the orientation angle of each individual polygon segment is measured. Finally the position (MD-, CD- and z-coordinate) and the orientation angle of each fiber segment are compiled to a three dimensional model of layered fiber orientation.



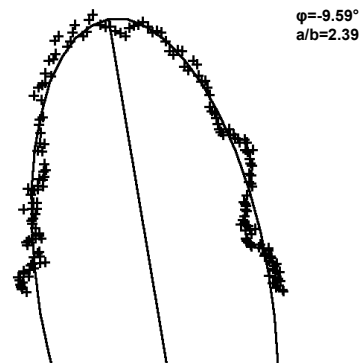
(a) A $10 \times 7 \text{ mm}^2$ part of a split paper sample



(b) The evaluated fibers (green) in subareas (red) of size $3.6 \times 3.6 \text{ mm}^2$



(c) Frequency distribution of the fiber segments measured within an area of $3.6 \times 3.6 \text{ mm}^2$ of 44 g/m^2 newsprint.



(d) Ellipse with rotation angle $\varphi = 9.59^\circ$ and anisotropy $a/b = 2.39$ fitted to FO distribution (c).

Figure 6 Fiber orientation measurement with image analysis. Fiber parts shorter than $170 \mu\text{m}$ are discarded from the measurement.

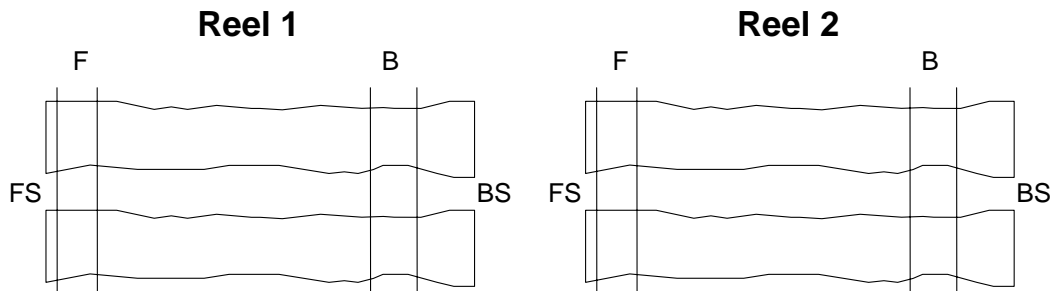


Figure 7 In an industrial trial on 80 g/m^2 copy paper with curl problems the effects of changes in the forming section were investigated. Between production of two reels the forming conditions were changed. From each reel samples were taken at the front side F and near the back side B. Curl on position F was stronger than on position B, see figure 8.

From this model the fiber orientation distributions of arbitrary 3-dimensional regions can be chosen. All the fiber segments within the selected region of the model are accumulated to a histogram with an angular resolution of 1° , see figure 6(c). This histogram represents the fiber orientation distribution of all the fiber segments within the selected regions of the sheet. In image 6(c) the FO distribution comprises all fiber segments measured within $3.6 \times 3.6 \text{ mm}^2$ of a 44 g/m^2 newsprint. It should be mentioned at this point, that it is also possible to calculate the fiber orientation distributions of z-directional fractions of the paper, for example the FO in the top 40% of the sheet. Finally fiber orientation angle and anisotropy of the distribution is calculated by fitting an ellipse to the FO distribution, see 6(d). The orientation of the ellipse's major axis is the FO angle and the ratio of ellipse's major- to minor axis length is the anisotropy of the fiber orientation.

4 Analyzing Curled Copy Paper

Copy paper (80 g/m^2) with strong CD- and diagonal curl from a commercial paper machine was investigated. The paper was produced on an older machine with a production speed of 800 m/min which had been upgraded with a hybrid former, a dilution headbox and turbulence vanes. A machine trial had been performed which lead to changes in the curl behavior of the paper. In this trial only changes in the forming section were made, slice lip profile and jet impingement was adjusted. Wet pressing, drying and furnish remained unchanged. It was the aim of the analysis to find out if the paper curl was related to fiber orientation.

The experiment is schematically outlined in figure 7. Paper from two different reels was analyzed, reel 1 was produced before the changes in the forming section, reel 2 afterwards. From each of the reels the samples were taken at two different cross directional positions. Position F

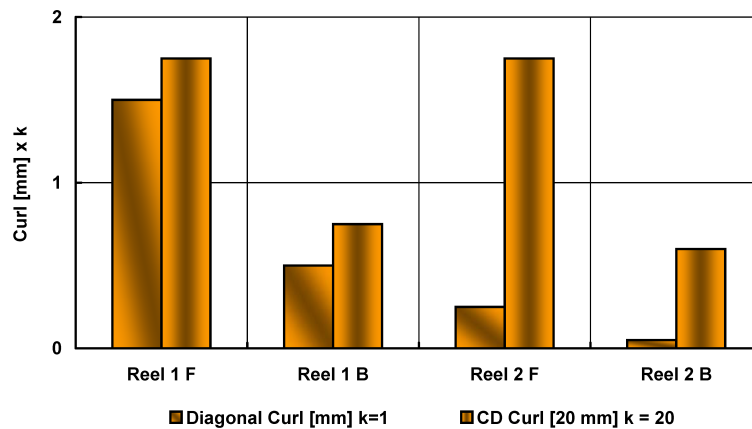


Figure 8 Diagonal curl (columns with diagonal pattern) mainly occurs in reel 1, i.e. before change of the forming conditions. CD curl (vertical pattern) occurs mainly on position F, but it persists after the changes in the forming section.

is directly at the front side edge of the web, position B is roughly 80 cm inside from the back side. So a total of four sampling positions was examined, two reels with two CD positions in each case.

Curl was measured in the paper mill. The values were determined independently for diagonal- and CD curl, see figure 8. At position F strong CD and diagonal curl appeared on reel 1, both values exceed production tolerances. After changes in the forming section (reel 2) the diagonal curl has improved remarkably whereas the CD curl had remained strong. The situation in position B is similar, only that the level of curl is generally lower. Diagonal curl improves from reel 1 to reel 2, CD curl persists. So it seems that the changes in forming conditions were beneficial for diagonal curl, but not for CD curl.

As outlined in section 1 two-sidedness of fiber orientation and hygroexpansivity of the paper are the main reasons for curl. Fiber orientation was determined with the sheet splitting based z-directional FO measurement described in the previous section. Hygroexpansivity of the paper was analyzed using an ultrasonic sheet tester. This instrument determines the elastic modulus of the paper, which is closely related to drying shrinkage and thus hygroexpansivity.

Hygroexpansivity. Hygroexpansivity of paper is closely related to the extent of drying shrinkage. The elastic modulus in the paper also depends on the drying shrinkage, it is lower if more drying shrinkage occurs. So there is an indirect relationship between the elastic modulus of paper and its hygroexpansivity, they are both largely determined by drying shrinkage. In fact that relationship is so strong that hygroexpansivity of paper can actually be calculated from the elastic modulus measured with an ultrasonic sheet tester [LINDBLAD & FÜRST 2001]. The quantitative relation is

$$H_{CD} = \frac{3.3}{TSI_{CD}} - 0.04 \quad (3)$$

where H_{CD} is the hygroexpansivity in machine cross direction and TSI_{CD} is the elastic modulus (also called tensile stiffness index TSI) in CD which is measured with the ultrasonic instrument. Using this equation the hygroexpansivity in CD was determined for all paper samples. Also MD hygroexpansivity was determined with equation (3), finally total hygroexpansivity was calculated as the average of MD and CD hygroexpansivity. The results are given in figure 9. Surprisingly the values are nearly equivalent for all sample papers. Usually CD hygroexpansivity is considerably higher towards the edges of the paper web, because CD drying shrinkage is much more intense in this region. According to these results there are no variations in the hygroexpansivity of the paper, which could explain the differences in the curl.

Z-directional fiber orientation. From each sampling point on the paper four specimen with an area of $3.6 \times 7 \text{ cm}^2$ each were analyzed. The samples were split and a 3D layered fiber orientation FO model was extracted. For this application local fiber orientation was not relevant, so only the z-directional FO was evaluated, see figure 10. Each of the plots refers to one sampling point, the top row shows the z-directional FO for reel 1, bottom row reel 2. Each figure contains four blue lines indicating the FO angle and four red lines indicating the FO anisotropy across the z-direction of the sheet. One line represents one of the specimen. The most remarkable result of this analysis is a distinctive FO angle two sidedness in position F of both samples. FO angle is around $+20^\circ$ in the bottom side of the sheet but it turns to -25° in the topmost 25% of the sheet, combined with a pronounced rise in anisotropy. On reel 1 (position F) about 25% of the sheet have a negative FO angle, on reel 2 (position F) only 12%.

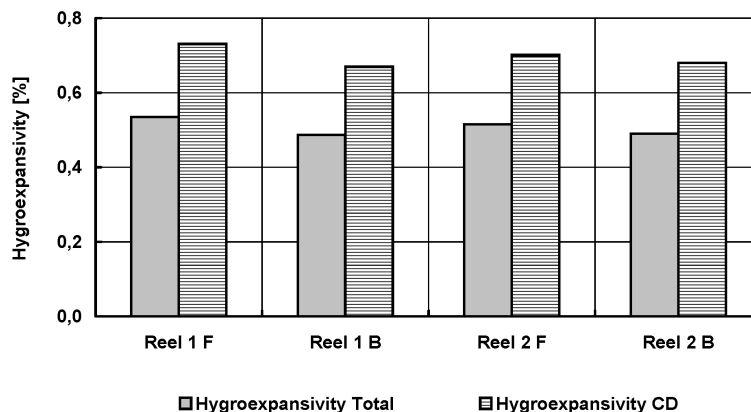


Figure 9 Hygroexpansivity calculated from ultrasonic sheet testing (TSI) data. Hygroexpansivity is roughly equivalent on both reels. More surprisingly it is also equivalent at the positions F (at the front side web edge) and B (somewhat inside the back side web edge).

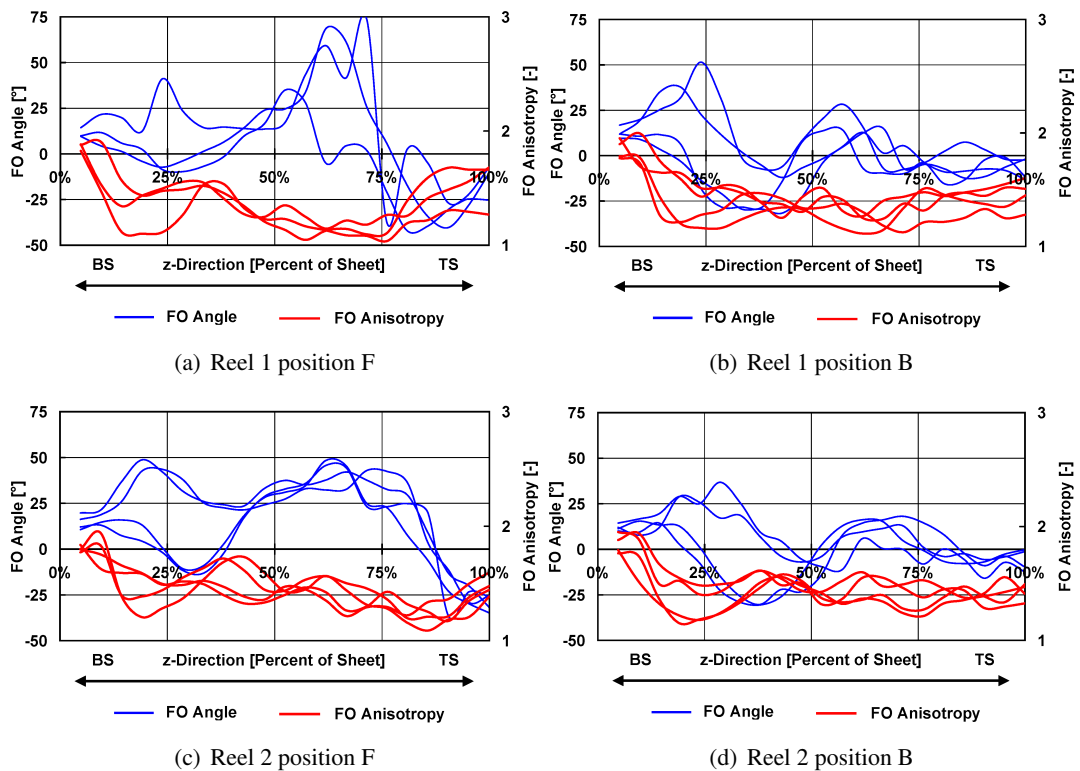
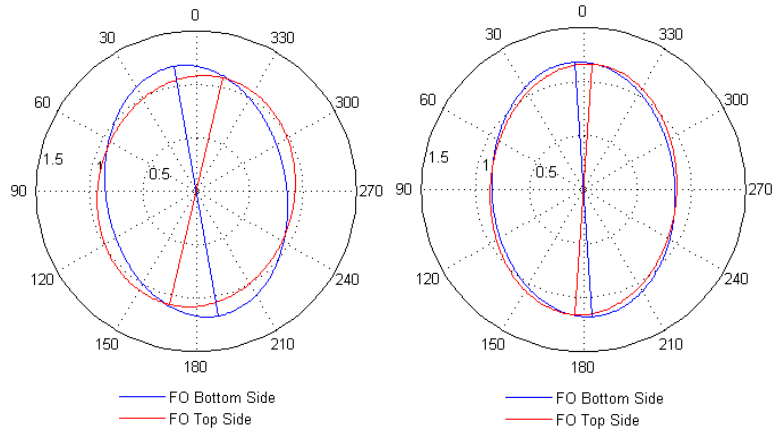


Figure 10 Fiber orientation across the z-direction of the sheet. FO angle is printed blue, FO anisotropy red. The x-axis gives the position in the cross section of the sheet, it runs from the bottom side BS to the top side TS. Please note the abrupt change in the FO angle towards the top side in position F on both reels (a and c).

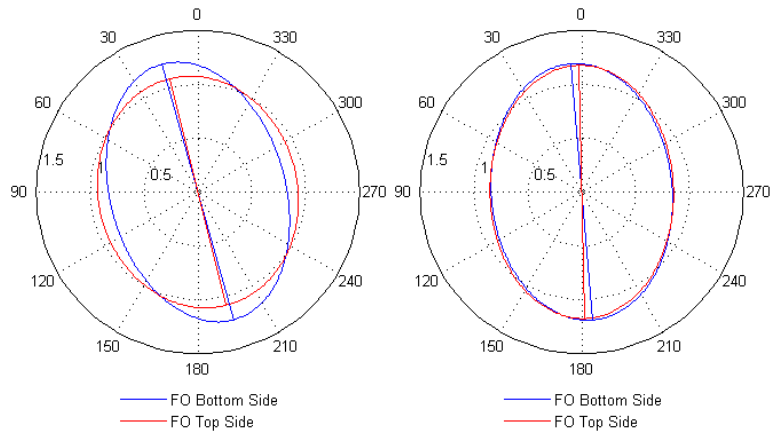
So FO angle two-sidedness in position F is - although still pronounced - considerably lower for reel 2. On position B fiber orientation is generally more even across the sheet and no evident two-sidedness can be observed.

A more condensed evaluation of the same data gives figure 11. For these plots the top 40% of fiber segments were aggregated to a top side FO distribution, an ellipse (red) was fitted to this distribution to quantify FO angle and anisotropy. Equivalently the FO distribution of the bottom 40% (blue) of the sheet was evaluated. For each of the plots a total sample area of 80 cm² was analyzed, so these plots represent the FO on a large scale. Evidently reel 1 position F exhibits strong angle two-sidedness which explains the strong diagonal curl. Also there is considerable FO anisotropy two sidedness in position F on reel 1 and 2, explaining the persisting CD curl. On position B only little two sidedness for both, FO angle and anisotropy is measured on both reels. That coincides with the substantially lower curl in that CD position of the web.



(a) Reel 1 position F: Strong two sidedness for FO angle and anisotropy, strong CD curl and diagonal curl.

(b) Reel 1 position B: Small FO angle two sidedness, no FO anisotropy two sidedness. Small diagonal curl, no CD curl.



(c) Reel 2 position F: No FO angle two sidedness, strong FO anisotropy two sidedness. No diagonal curl, strong CD curl.

(d) Reel 2 position B: No two sidedness for FO angle and anisotropy, no CD curl and diagonal curl.

Figure 11 Fiber orientation two-sidedness. Fiber segments from the top- respectively the bottom 40% of the 3D-FO model were aggregated, then ellipses were fitted to the FO distributions. Please note that the fiber orientation two sidedness agrees well with the intensity of diagonal curl and CD curl (see figure 8) according to the theory described in section 1.

In a qualitative way, for the examined paper samples the fiber orientation two sidedness agrees with the curl according to the theory outlined in section 1. This is also summarized in figure 11.

5 Quantitative Modeling of Curl Intensity

The measurements of z-directional fiber orientation and hygroexpansivity have already indicated, that fiber orientation is probably the reason for the observed curl differences. Now quantitative models of the observed curl based on the expressions for diagonal curl (equation 1) and CD curl (equation 2) are presented.

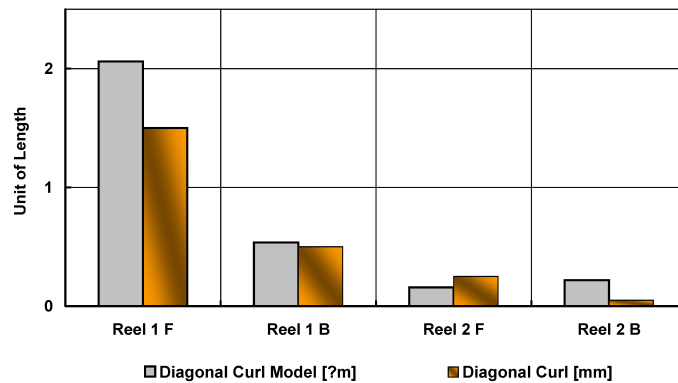
Both expressions, for diagonal curl and for CD curl, consider sheet thickness t in their denominators. As all the analyzed papers had the same caliper, the value of t was not considered for the models. Furthermore the results of the models can not be interpreted as absolute values because fundamental constants like the modulus of elasticity or sheet size for curl measurement were not evaluated quantitatively. Thus the model results have an unspecified unit of length.

Diagonal curl. Using the results for total hygroexpansivity H , figure 9 and fiber orientation angles ϕ_{TS} and ϕ_{BS} of the top- respectively the bottom side of the sheet, figure 11, it is straightforward to calculate diagonal curl intensity K_{xy} from equation (1). Figure 12(a) shows the result from this calculation as well as the actually measured diagonal curl values. Agreement between model (grey columns) and measured values (orange columns) is good. As hygroexpansivity is identical for all samples, the calculated curl depends only on fiber orientation angle two sidedness which is displayed in figure 11. FO angle two sidedness on reel 1 position F is high, it is considerably lower on Reel 2 position F. There is hardly any FO angle two sidedness at position B on both reels.

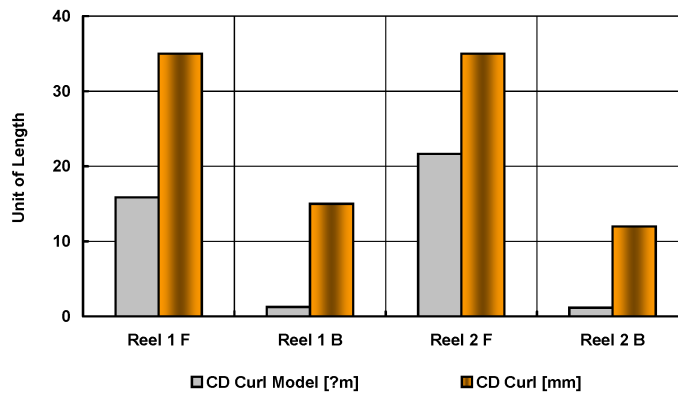
Calculation of **CD curl** requires some adjustments of equation (2). Hygroexpansivity ε was not measured for different layers of the sheet. For our CD curl model we will only consider two sidedness of FO anisotropy because this is the major influence factor for differential CD shrinkage [KAJANTO & NISKANEN 1998]. Accordingly the difference in CD strain ($\varepsilon_{CD}^{TS} - \varepsilon_{CD}^{BS}$) is substituted by $H_{CD}(A_{TS} - A_{BS})$. Here H_{CD} is the hygroexpansivity in CD as it was calculated from ultrasonic measurement and A_{TS} respectively A_{BS} are fiber orientation anisotropy on the top and bottom side of the sheet.

$$K_y = \frac{2(\varepsilon_{CD}^{TS} - \varepsilon_{CD}^{BS})}{t} \approx \frac{2H_{CD}(A_{TS} - A_{BS})}{t} \quad (4)$$

This approximation for CD curl by FO anisotropy two sidedness is obviously only valid, if the FO of the examined paper is aligned in MD, which should be true in most of the cases. The results of the CD curl model as well as the measured curl values are displayed in figure



(a) Diagonal curl, the modeling was performed according to equation (1).



(b) CD Curl, the modeling was performed according to equation (4).

Figure 12 Comparison between the results of quantitative curl modeling (grey columns) and actually measured data of 80 g_m² copy paper from an industrial paper machine (orange columns). Diagonal curl (a) and CD curl (b) were independently modeled for the same papers.

12(b). Agreement is quite good. Sheets from position F have strong CD curl on both reels, not so sheets from position B. Again only fiber orientation is responsible for the differences, because results for hygroexpansivity were equivalent. Figure 11 demonstrates that the position F exhibits a distinct FO anisotropy two-sidedness for both reels, which can not be observed for position B.

Although the introduced models for diagonal curl and CD curl contain major simplifications, they worked well for the examined specimen. Still only a few sample papers were examined, for a general verification much more samples need to be analyzed. Modeling of diagonal curl based on fiber orientation angle two-sidedness and hygroexpansivity was also performed by [FEICHTINGER 1996]. In a large scale laboratory trial he found a good correlation to his model, which confirms the applicability of equation (1) for quantitative analysis of curl.

6 Conclusions

Originating from theoretical formulations of paper curl a method was outlined to quantify the influence of fiber orientation on diagonal curl (twist curl) and CD curl. The key point is, that diagonal curl and CD curl are affected by fiber orientation in a different manner. The former descends from FO angle two-sidedness, that latter may be caused by FO anisotropy two-sidedness.

A semi quantitative model of CD-curl and diagonal curl based on fiber orientation in z-direction of the sheet and paper hygroexpansivity well described the behavior of industrial paper samples. Specifically the model explained well, why diagonal curl in the industrial papers disappeared, whereas CD curl prevailed.

Although the data presented here certainly is too limited to validate the model for general applicability, it still seems to be useful to analyze the effect of fiber orientation on curl.

References

- Carlsson, L., Fellers, C. & Htun, M. [1980], 'Curl and two-sidedness of paper', *Svensk Papperstidning* **83**(7), pp. 194–197.
- Erkkilä, A., Pakarinen, P. & Odell, M. [1998], 'Sheet forming studies using layered orientation analysis', *Pulp and Paper Canada* **99**(1), pp. 81–85.
- Feichtinger, M. [1996], Über die Auswirkung der Faserorientierung in Papieblättern, PhD thesis, Graz University of Technology.
- Green, C. [2000], 'Curl in paper', *Appita J.* **53**(4), pp. 272–275.
- Hirn, U. [2006], New Methods in Paper Physics Based on Digital Image Analysis, PhD thesis, Graz University of Technology.
- Hirn, U., Bauer, W. & Wiltsche, M. [2004], Lokale Faserorientierung und ihr Einfluss auf kleinflächige Planlagestörungen, in H. Runge & R. Sangl, eds, '16th PTS-Symposium 2004 Chemical Technology of Papermaking', München, pp. 37.1 – 37.14.
- Juppi, K. & Kaihovirta, J. [2003], 'The effect of the dryer section on paper quality', *Pulp and Paper Canada* **104**(5), pp. T131–T134.
- Kajanto, I. & Niskanen, K. [1998], *Dimensional Stability - Curl*, Vol. 16 - Paper Physics of *Papermaking Science and Technology*, Fapet Oy, chapter 7, pp. 239–251.
- Knotzer, U., Wiltsche, M. & Stark, H. [2003], 'Papierstruktur in z-Richtung', *Wochenblatt für Papierfabrikation* (12), pp. 688–699.
- Levlin, J.-E. & Söderhjelm, L., eds [1999], *Pulp and Paper Testing*, Vol. 17 of *Papermaking Science and Technology*, Fapet Oy. ISBN 952-5216-17-9.
- Lindblad, G. & Fürst, T. [2001], *The Ultrasonic Measuring Technology on Paper and Board*, Lorentzen and Wettre. ISBN 91-973781-0-0.
- Lloyd, M. & Chalmers, I. [2001], 'Use of fibre orientation analysis to investigate sheet structural problems during forming', *Appita J.* **54**(1), pp. 15–21.
- Morris, V. & Sampson, W. [1998], 'An investigation of heat curl in newsprint', *Tappi J.* **81**(8), pp. 191–194.

- Nemeth, M., Kole, D. & Hellström, A. [1999], Papermaking applications using new online fiber orientation measurement, in 'Proceedings of the 53rd Appita Annual Conference', pp. 709–712.
- Niskanen, K. [1993], 'Anisotropy of laser paper', *Paperi ja Puu* **75**(5), pp. 321–328.
- Odell, M. & Pakarinen, P. [2000], The complete fibre orientation control - and diverse effects on paper properties, in 'XII Valmet Paper Technology Days', pp. 20–41.
- Parker, J. & Mih, W. [1964], 'A new method for sectioning and analyzing paper in the transverse direction', *Tappi J.* **47**(5), pp. 254–263.
- Shands, J. & Genco, J. [1988], 'Cross machine variation of paper curl on a twin wire machine', *Tappi J.* **71**(9), pp. 165–169.
- Viitaharju, P. & Niskanen, K. [1994], 'Chiral curl in thin papers', *J. Pulp and Paper Sc.* **20**(5), pp. J148–J152.